Mechanical and Thermal Properties of CU-Infiltrated P/M Tungsten Nozzles

Shu-En Hsu,* Chung-I Chen,† Shen Yue,† and Franz Kong-Wen Li‡
Chung-Shan Institute of Science and Technology, Taiwan, Republic of China

Tungsten nozzles made of sintered powder with copper infiltration have a good combination of strength, ductility, resistance to erosion, and fracture toughness. Powder metallurgy (P/M) combined with a process of infiltration produces a fine W-Cu composite which cannot be produced by conventional metallurgical processes. The effects of varying environmental parameters on sintering and infiltration processes are discussed. The mechanical and thermal properties of the W-Cu composite nozzle are shown. Density measurement and microstructure analysis after testing reveal redistribution of infiltrated copper which qualitatively explains the functioning of transpiration cooling.

I. Introduction

SIGNIFICANT efforts are being made to fabricate high-performance nozzles for rocket propulsion. One of the most serious problems in the uncooled solid propellant motor is to find proper materials for the nozzle insert. The throat area of the nozzle is subjected to maximum heat flux, maximum thermal shock, and maximum erosive attack without regenerative cooling. Among the refractory materials available, tungsten and graphite have proved to be the best for nozzle inserts. Of the two, tungsten has much better erosion resistance and is particularly preferred for multiple nozzle motors where the erosion rate is critical and the throats are moderately small. As early as 1958, tungsten had already been tested as a rocket insert.[1] It was found that neither "cold" nor "hot" pressing methods produced tungsten with adequate strength, erosion resistance, and thermal shock resistance to withstand the extreme thermal stress environment encountered in rocket nozzles.[2] One recent approach is the development of a porous tungsten matrix that could be infiltrated with ductile metal of lower melting point. The concept of using infiltrated tungsten for rocket nozzles includes utilization of an infiltrant with a boiling point below the operating temperature of the nozzle so as to carry heat away from the nozzle throat surface by transpirating cooling. Silver has been used as the infiltrant.[3]

The objective of our efforts is to improve the fabrication processes to produce copper infiltrated tungsten nozzles with reliable performance. The results of static test firings of nozzles with copper infiltrated tungsten inserts were acceptable. The copper infiltrated tungsten composite has excellent machinability as well as a superior combination of high strength, resistance to erosion, and thermal shock.

II. Experimental Procedure

Sample Preparation

Green Compact—tungsten powder, 325 mesh, with purity of 99.9% was obtained from the Ventron Co. (U.S.A.). Figure 1 shows the SEM photographs of tungsten powder which is produced by the hydrogen reduction technique.

The reduction cycle is controlled to produce powder with desired particle shape and size. Different particle sizes of tungsten powder were tested in the sintering process. It was found that porosity was difficult to control in powders with average particle size less than 3μ while powders with average particle size greater than 7μ did not retain the infiltrant in the pores due to insufficient capillarity.

Prior to forming, the tungsten powder was mixed with benzene solution (20cc/100gr) and 1.5wt% paraffin and then blended for 24 hours to ensure green compact strength and uniform particle distribution. After blending, the mixture was baked to dry and loaded into a steel mold. Consolidation was done either manually or semiautomatically with a 100-ton powder press. For small size nozzles, hot or isostatic pressing is not needed. The optimum forming pressure was about 6 ton/cm^2 to ensure green density of 65% of theoretical density.

Sintering—the green compact was dewaxed at 600°C for one hour. To avoid the possibility of oxidation, the dewaxing process was carried out in an argon atmosphere furnace. Upon completion, the green compact was placed in the sintering furnace as quickly as possible. A graphite resistance furnace from Astro Industries, Inc., was utilized for sintering. Vacuum and hydrogen furnace atmospheres were tried. When a hydrogen atmosphere is used, hydrogen should be dried and purified before entering the furnace. The hydrogen will tend to reduce any oxide that is present. The rate of oxide reduction depends on the pore area, rate of vapor-transpiration, and purity of hydrogen. A disadvantage of hydrogen is that it reacts with graphite at temperatures above 1500°C to form methane, CH_4, which in turn reduces the oxide, producing free carbon and water vapor. The latter becomes an active agent in the oxidation-reduction cycle, while the former reacts with tungsten at high temperature to form a thin layer of carbide skin on the compact specimen, which is clearly undesirable due to its extreme hardness and

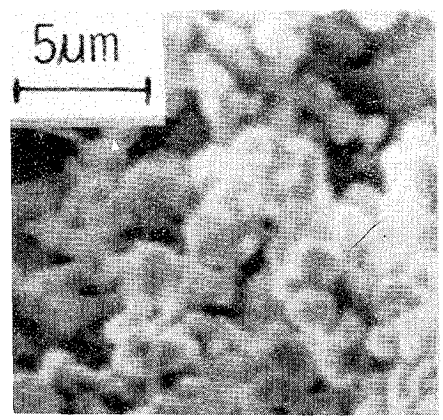

Fig. 1 SEM metallograph.

Presented as Paper 76-712 at the AIAA/SAE 12th Propulsion Conference, Palo Alto, Calif., July 26-29, 1976; submitted Aug. 23, 1976; revision received Nov. 17, 1976.
Index category: Materials, Properties of.
*Senior Scientist.
†Assistant Scientist.
‡Associate Scientist.

poor machinability. For this reason, the sintering process in our studies was conducted in vacuum in which only a negligible oxide layer covering the tungsten particles is formed.

The heating cycle of sintering is illustrated in Fig. 2. There are two plateaus in the heating curve. The first one, at 750°C, is held for a short time for the purpose of retaining the desired degree of vacuum, which was influenced by evacuation of paraffin gas during heating. The second one, kept at 1800°C for two hours, ensured completeness of sintering.

Infiltration—the sintered tungsten nozzles, with desired density of 73-82% of theoretical, were reloaded into the Astro graphite resistance furnace for copper infiltration. The green density of 65% of theoretical leads to 75% sintered density in our sintering condition. The range of 73-82% is due to the variation of size and shape of the particles. The specimens were set in a graphite suscepter with flat bottom, copper powder was paved in between the specimens and the bottom to avoid direct contact with graphite, and flakes of infiltrant copper were put onto the specimens. The infiltration process was conducted in hydrogen at 1390°C (melting point of copper is 1083°C). Rate control in infiltration is important; if the infiltration rate is too fast or control of infiltration direction is improper, the reverse pressure which builds up due to the trapped gases will prevent further infiltration. The heating curve for copper infiltration is also shown in Fig. 2. In the heating cycle, temperature is held at 950°C for one hour prior to reaching the melting point of copper, allowing hydrogen to penetrate the pores of the tungsten matrix to reduce the oxide; otherwise, the oxide will retard the rate of infiltration.

Mechanical and Thermal Tests—the copper-infiltrated composites were machined to the desired shape of nozzle insert. Prior to inserting the multiple nozzles into the holder, a layer of Al_2O_3-ceramic powder was plasma-sprayed on the surface of the inserts. To ensure strong bonding between the nozzle inserts, and the back up of ceramic, a serrated surface was machined around the nozzle. The nozzles at different stages of fabrication are shown in Fig. 3.

Thermal conductivity of the copper-infiltrated tungsten nozzles was tested by using Tcfcm-N20 of Dynatch Corp. The samples were in the shape of 1 in. diam, 0.5 in. high and then were cut and polished for metallographic analysis and density measurement. The mechanical compression tests were carried out by 10t Instron with crosshead speed equal to 0.2 cm/min. The sample was in the shape of 4.8 mm diam × 7 mm. The loading surfaces were machined to fit the loading plates. Between the loading surfaces and loading plates some waterproof lubricant were spreaded. Some cracks turned out on the surface parallel the axis of sample after loading. Barrelling was also observed.

III. Results and Discussion

Green Compact Properties of Tungsten—green compact density as a function of forming pressure is shown in Fig. 4.

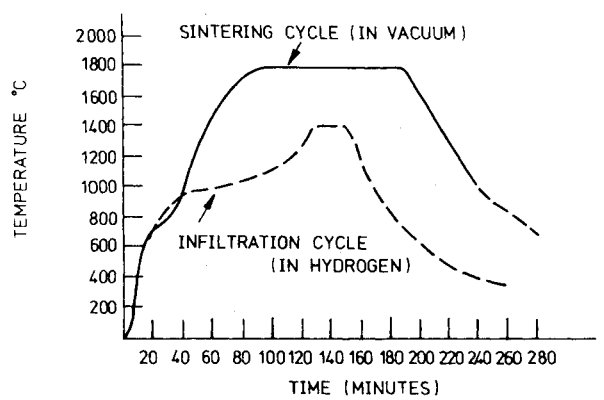

Fig. 2 Heating cycle of sintering and infiltration.

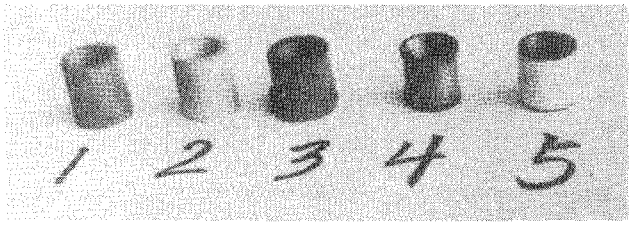

Fig. 3 Tungsten nozzle inserts made by P/M process and Cu-infiltration: 1) green compact; 2) as-sintered; 3) as-Cu-infiltrated; 4) as-machined; and 5) as-Al_2O_3-sprayed.

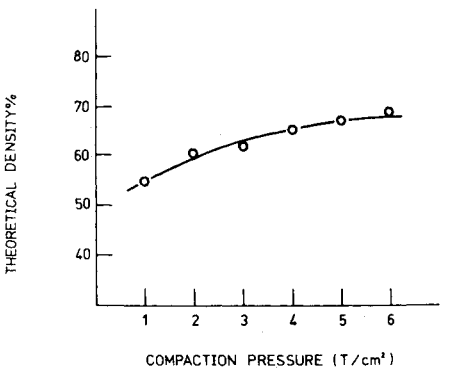

Fig. 4 Pressed density as a function of compaction pressure.

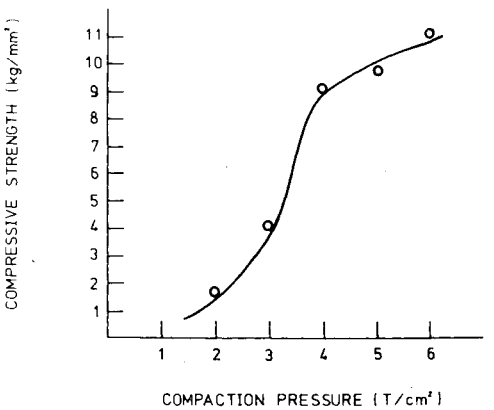

Fig. 5 Pressed compressive strength as function of compaction pressure.

Density goes up as forming pressure increases. When the pressure reaches 6 ton/cm^2, green density is close to saturation, i.e., about 65% of theoretical density. By this green density the proper quantity of copper can be infiltrated into the pores of tungsten matrix. Compressive strength of the green compact depends primarily on green compact density. As shown in Fig. 5, compressive strength increases rapidly in the pressure range of 3 to 4 ton/cm^2. This probably results from a drastic change in alignment between particles. The formability of tungsten powder is much lower than that of other metal powders. Iron powder, for instance,[4] can be compacted to 92% of theoretical density (but mostly only 85-90% by using commercial powders) at the pressure of 6 ton/cm^2. The poor formability of tungsten powder is due to[5] its small, hard, and brittle particles with roughly spherical shape, less interlocking and high friction during pressing. Figure 6 gives the SEM metallographs of the green compact of tungsten.

Sintering Characteristics of Tungsten Powder—Fig. 7 shows the influence of sintering atmosphere on the sintered density—forming pressure. The green compact density is also shown for comparison. It is noted that the density sintered in vacuum is higher than in hydrogen. This situation remains the

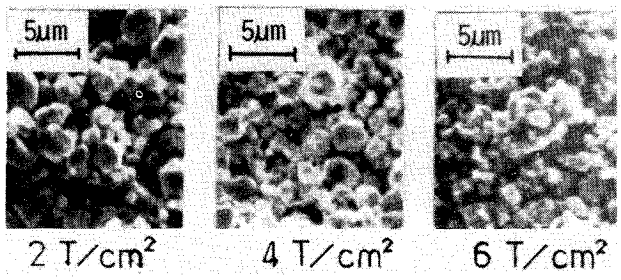

Fig. 6 SEM metallographs of the green compact at three different pressures.

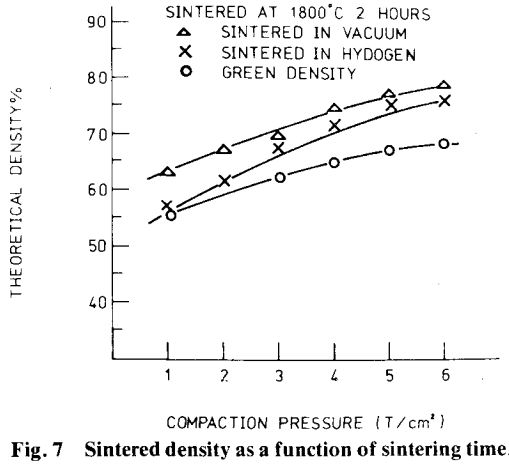

Fig. 7 Sintered density as a function of sintering time.

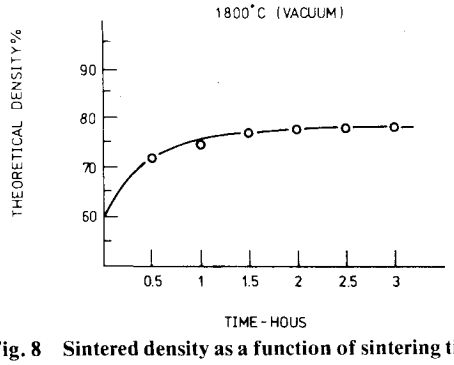

Fig. 8 Sintered density as a function of sintering time.

same even after copper-infiltration. The relation between sintered density and sintering time is given in Fig. 8. As the figure shows, the density increases gradually until the curve turns out to be flat after 1½ hours. Although longer sintering time has little effect on the sintering density, this is not the case for sintered strength. Figure 9 illustrates the influence of sintering time on compressive strength at various sintering conditions. It is obvious that sintering in vacuum is much better than in argon. In order to obtain the desired density 73-82% of theoretical density for copper infiltration, the optimum conditions for tungsten sintering are: compression pressure = 6 ton/cm^2; sintering atmosphere = vacuum; sintering temperature 1800°C; and sintering time = 2 hours. The sintering time of two hours is sufficient for keeping good strength.

Infiltration—infiltration is carried out at 1390°C, 307°C above the melting point of copper. This infiltration temperature was selected experimentally. By 1390°C the infiltrant was reaching a maximum, about 39.87g in our case. Below or above this temperature the quantities become less. It seems that at this temperature the liquid copper exhibits enough viscosity to keep equilibrium with capillary force of the matrix. After infiltration the excess copper around the base of the nozzle can be removed easily be machining.

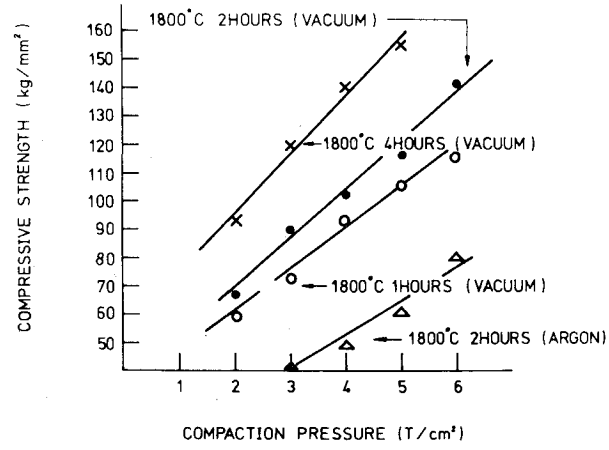

Fig. 9 Influence of sintering time on compressive strength as a function of compaction pressure.

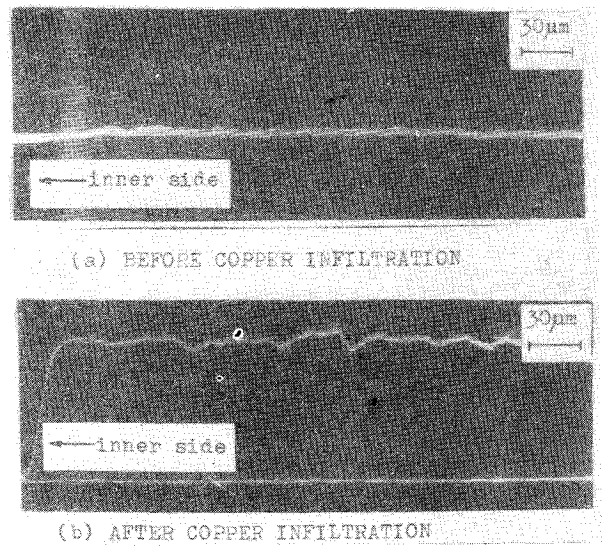

Fig. 10 Comparison of copper distribution across tungsten nozzle throat.

A Y-modulation device attached to the SEM displays semiquantitatively the distribution of an element along a scanned line across the sample. Figure 10 compares the distribution of copper along a line scan across the nozzle throat before and after copper infiltration. Density measurement shows that 94% of the pores in the tungsten matrix were filled with copper.

The compressive true stress-true strain curve of the Cu-infiltrated tungsten is shown in Fig. 11. The composite is so ductile that almost no evidence of fracture was found even when deformed to 60% strain. The ductile behavior of the Cu-infiltrated tungsten nozzle provides an excellent combination of thermal shock resistance and machinability.

Figure 12 gives the comparison of 0.2% offset compressive yield strength between the Cu-infiltrated and as-sintered specimens at different compact pressures. Again, specimens prepared at the following conditions demonstrate excellent performance: compact pressure = 6 ton/cm^2; sintering atmosphere = vacuum; sintering temperature = 1800°C; sintering time = 2 hours; infiltration atmosphere = hydrogen; infiltration atmosphere = 1390°C; infiltration time 1 hour. The metallograph of Cu-infiltrated tungsten is shown in Fig. 13.

Rocket Test—characteristics of the Cu-infiltrated tungsten nozzle are: bulk density = 16.58 g/cm^3; melting point of tungsten matrix = 3410°C; melting point of infiltrant, copper = 1083°C; boiling point of infiltrant, copper = 2600°C;

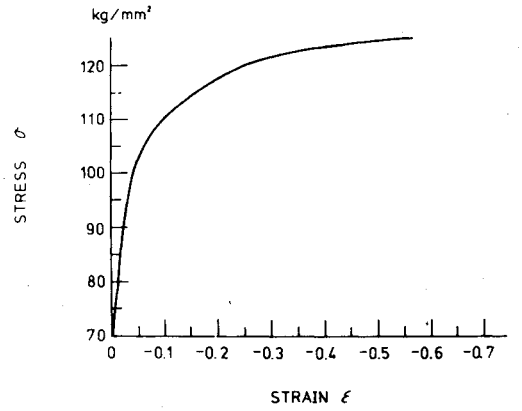

Fig. 11 True strain-stress diagram of Cu-infiltrated tungsten.

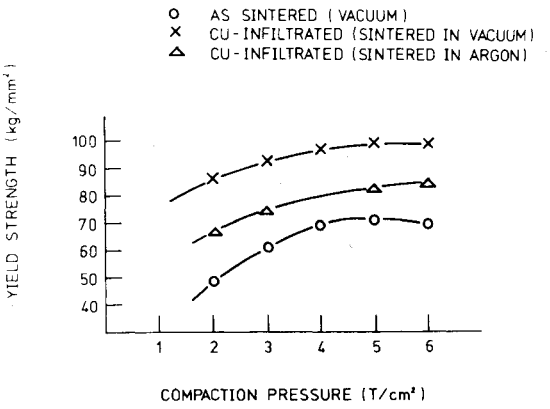

Fig. 12 Comparison of strength of Cu-infiltrated tungsten and as-sintered tungsten.

heat of fusion of copper[6] = 50.65 cal/g; heat of evaportion of copper[7] = 72.8 k-cal/g-atom; thermal conductivity of W-Cu composite (at 380°C) = 91.2 Btu/hr-ft-°F; and compressive strength = 92 kg/mm^2.

The copper-infiltrated tungsten nozzles have been successfully tested in static test firing. It was carried out on a fixed stand. There are 7 nozzle inserts in the booster. The burning time for the booster is about 4 sec.

It is significant to note in Table 1 that the average erosion rate of the CU-infiltrated tungsten nozzle inserts exhibits negative values. This means that the diameter of the nozzle inserts shrinks after test firing. In order to check whether the shrinkage of the throat diameter is due to expansion of the tungsten matrix or is due to the deposition of solidified SEM. A photograph showing redistribution of copper scanned across the throat area is illustrated in Fig. 14. Note that the infiltrated copper near the surface of the throat was depleted, indicating that shrinkage of the inner diameter of the nozzle is entirely due to expansion of the tungsten matrix. And the dilitation is possible only near the inner boundary, because there is no way to go near the outer boundary. Whether this would lead to very high circumferential stresses in the outer

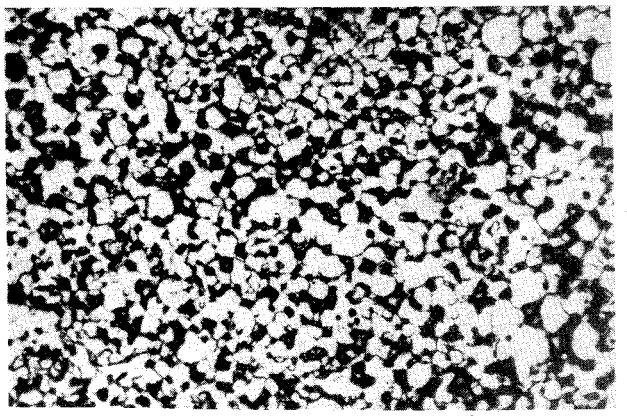

Fig. 13 The metallograph of Cu-infiltrated tungsten (770x).

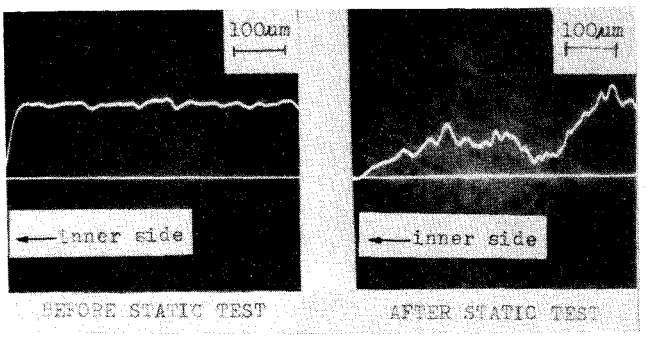

Fig. 14 Comparison of redistribution of infiltrated copper across nozzle throat before and after static test firing.

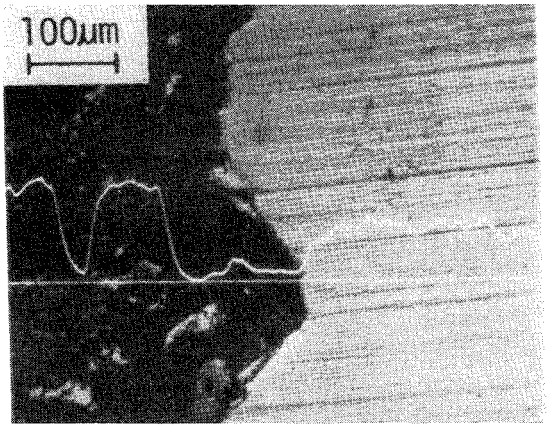

Fig. 15 Copper distribution across ceramic back-up after static test.

part of the nozzle remained to be further studied. Because of the high resistance to erosion the test motor maintained an extremely stable chamber pressure throughout burning.

For the purpose of detecting the function of transpiration cooling of the infiltrant copper, a display of copper distribution scanned across the backup Al_2O_3-ceramics is

Table 1 Erosion resistance of Cu-W insert

Rocket condition Propellant: AP + polyester				Erosion data (average of 10 tests)			
Combustion temperature °C	Chamber pressure MN/M^2	Burning time sec	Number of nozzle inserts	Bulk density before test g/cm^3	Bulk density after test g/cm^3	Density loss rate g/cm^3-sec	Average erosion rate mm/sec
2700	108	4	7	16.58	15.98	0.15	−0.028

shown in Fig. 15. As shown in this figure, some infiltrated copper has diffused out of the tungsten matrix into the ceramic during the melting stage. Apparently, significant heat has been removed by mass transpiration.

Copper has a higher boiling point than silver (2200°C for Ag, 2600°C for Cu). Therefore it is expected that very little copper vaporized during test firing. They transferred to the liquid state first and then migrated onto the throat surface in the form of drops which were removed by the high rate flame. As a result, the throat area of the nozzle insert was cooled by transpiration, analogous to perspiration cooling of humans. Apparently transpiration cooling is a result of the liquefaction of copper.

IV. Summary

The important points in finding of the optimum conditions of manufacturing copper infiltrated tungsten nozzle inserts are now summarized: 1) Infiltration efficiency is controlled by particle size and shape. Porosity in the green compact of tungsten is a significant factor in the process of copper-infiltration. Density of the green compact of tungsten becomes saturated at consolidation pressure of 6 ton/cm^2. Powder metallurgy product having 65% theoretical density is satisfactory for sintering. 2) The sintering process can be completed in vacuum at 1800°C for two hours. The density of as-sintered tungsten is about 75% of theoretical density, which exhibits desired porosity for copper infiltration. 3) The copper infiltration process is conducted in hydrogen atmosphere at 1390°C for one hour. Density measurement and SEM scanning analyses show that 94% of the pores are infiltrated with copper. 4) Rocket static firing tests show that Cu-infiltrated tungsten nozzles made by powder metallurgy techniques exhibit an excellent resistance to thermal shock and erosion.

References

[1]Hove, J.E. and Riley, W.C., *Ceramics for Advanced Technologies*, Wiley, N.Y., 1965, Chap. 13.

[2]Hausner, H. H., Roll, H. H., and Johnson, P. K., *Perspective in Powder Metallurgy*, Vol. 3, Plenum, N. Y., 1968.

[3]Matt, R. E. and Warga, J. J., *Metallurgical Processing of Silver Infiltrated Tungsten*, Vol. 1, Gordon and Breach Science Publishers, Inc., N. Y., 1965.

[4]Mazyama, "Powder Metallurgy—Sintering Mechanisms," *Nikan Industrial News*, 1964.

[5]Poster, A. R., "Tungsten Powder—A New Engineering Material," *Precision Metal Molding*, Jan., 1962, p. 39.

[6]*ASM Metals Handbook*, 8th Edition, 1969, p. 46.

[7]Smithells, C.J., *Metals Reference Book*, Vol. 1, 4th Edition, Plenum Press, N.Y., 1967, p. 224.